

## Al계 준결정 분말의 제조 및 응용

제3회 최신분말제품 응용기술 workshop

2002. 7. 20

W. T. Kim  
Chongju University

Acknowledgements to D.H. Kim, S.M. Lee, E.Fleury, H.S. Ahn\*  
Center for Noncrystalline Materials, Yonsei Univ.,\*KIST



### Contents of talk

- 1) Introduction
  - Quasicrystals ?
  - General properties of quasicrystal
  - Potential application
- 2) Preparation of Al-Cu-Fe powders
- 3) Thermal spray coating for thick film
- 4) Experimental
  - Thermal coating : APS, HVOF
  - Tribological test
- 5) Results and discussion
- 6) Super-hard steel coating
- 7) Summary



## What is quasicrystals ?

- ▶ Crystal : periodic sharp diffraction pattern showing  
2, 3, 4, or 6 rotation symmetry  
Periodic distribution of atoms translation & rotation order
- ▶ Quasicrystals : sharp diffraction pattern but with aperiodic  
distribution of diffraction spots with 5, 8, 10 or 12-fold  
rotation axis  
Aperiodic distribution of atoms with rotation order
- ▶ Amorphous : diffuse halo pattern  
Random distribution of atoms

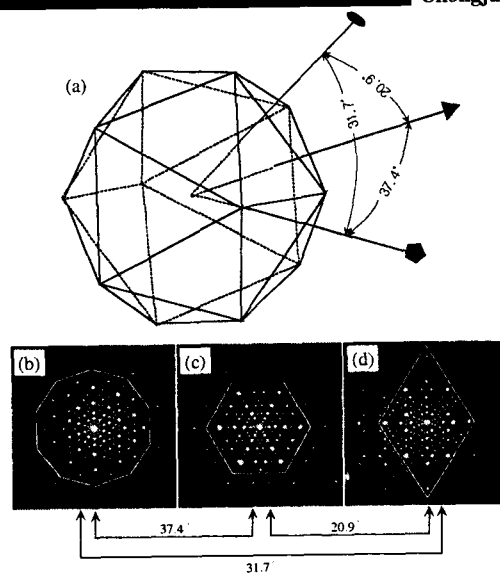
•1991, International Union of Crystallography  
"crystal" : *any solid having an essentially discrete diffraction diagram*



## Icosahedral phase

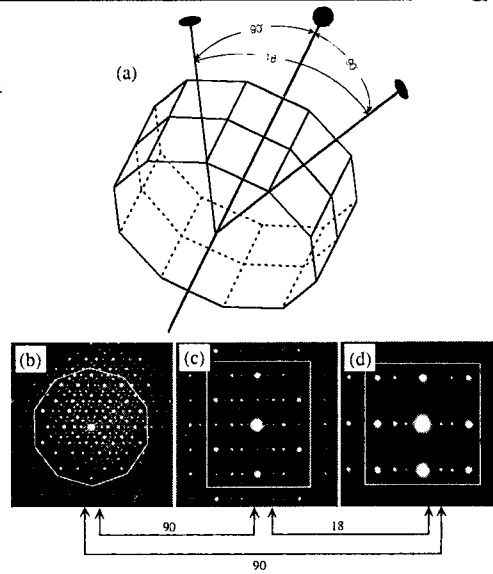
1984 by D. Schechtman  
Al-Mn alloy (RSP)

Stable I phase  
Al-Cu-Fe,  
Mg-Zn-Y,  
Ti-Ni-Zr etc.

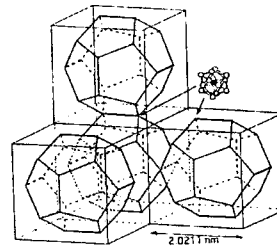
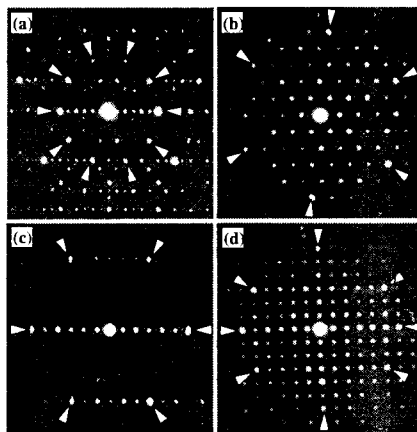


### Decagonal phase - 2D quasicrystal

Al-Ni-Co,  
Al-Cu-Co etc



### Cubic approximant phase in the Al-Cu-Fe-Si system



- (a) pseudo 5-fold axis
- (b) pseudo 3-fold axis
- (c) another pseudo 3-fold axis
- (d) pseudo 2-fold axis

### Comparison of properties of Quasicrystals with others

		Density (g/cm <sup>3</sup> )	Thermal conductivity (W/mK)	Thermal expansion (10 <sup>-6</sup> K <sup>-1</sup> )	Adhesion energy (mJ/m <sup>2</sup> )	Electrical resistivity (μΩcm)
Quasicrystals	Al-Cu-Fe	3.5-4.5	1.8	14-19	57-67	2500
	Al-Co-Fe-Cr	3.5-5.0	2.3-4.0	14-19	62-72	-
Metals	Al alloy	2.7	202-243	24	97.8	2.65
	Cu	9.0	387	17	105	1.7
	Steel	7.8	62-90	12-20	98	9.7
Ceramic oxides	Al <sub>2</sub> O <sub>3</sub>	3.5-3.9	3.4-3.5	8.4	120	>100000
	ZrO <sub>2</sub> + 8%Y <sub>2</sub> O <sub>3</sub>	5.6-6.0	1.8-2.7	7-9	-	>10000



### Comparison of properties of Quasicrystals with others

		Young's modulus (GPa)	Fracture strength (MPa)	Elongation at rupture (%)	Micro- hardness (kg/mm <sup>2</sup> )	Coefficient of friction
Quasicrystals	Al-Cu-Fe	130-140	250-690	0.35-1.10	715-750	0.12
	Al-Cu-Fe-B	140	595-1010	0.65-0.85	670-850	0.15
Metals	Al alloy	72	325	15.0	87	0.37
	Copper	130	235	45	48	0.42
	Low carbon steel	205	620	32	120	0.32
Amorphous alloys	Al-Zr-Ni	80.4	800	1.4	340	-
	Al-Y-Ni	71.2	1140	1.6	300	-



### Physical properties of Al-Cu-Fe icosahedral phase

- Young's modulus : 61-110 Gpa
- Elongation at fracture : 0.35-1.1 %
- Microhardness Hv : 7.15 GPa
- Thermal conductivity : 1.8 W/mK
- Thermal expansion coefficient : 14-19 x 10<sup>-6</sup> K<sup>-1</sup>
- Low friction coefficient : 0.05-0.4
- High corrosion resistance
- Electro-optical property
- Low surface energy : 24-25 mJ/m<sup>2</sup>
- Fracture toughness : 1 MPam<sup>1/2</sup>

### Physical properties of the Al-Ni-Co(-Si) decagonal phase

- ✓ Young's modulus : 165 GPa
- ✓ Elongation at fracture : 0.9 %
- ✓ Microhardness Hv : 8.3 GPa
- ✓ Thermal conductivity : 2-6 W/mK
- ✓ Thermal expansion coefficient : 14-19 x 10<sup>-6</sup> K<sup>-1</sup>
- ✓ Low surface energy
- ✓ Low friction coefficient
- ✓ Good oxidation/corrosion resistance
- ✓ Electro-optical property

## Potential application of I phase

- ▶ **Structural application**
  - Composite material consisting of ductile phase : ex-situ or in-situ
  - ▶ High-strength Al alloys : Al with I precipitation
  - ▶ Surgical tools, electric shavers : Maraging steel with I precipitation
  - ▶ Mg alloy strengthened by I phase
- ▶ **Functional application :**
  - Thin film or thick film applications :
    - Thermal barrier coating (low thermal conductivity)
  - ▶ **Wear resistance coating (low friction coefficient)**
    - ▶ Coating of powertrain tools
  - ▶ **Non-stick coating (low surface energy)**
    - ▶ Cookware
    - ▶ Non-stick, wear resistant tire mold coatings
    - ▶ Injection molding cavity surface enhancements

### Composites :

quasicrystalline particles + crystalline/amorphous matrix

### Fabrication :

PM method : Al-Cu-Fe + alloy powder

Casting : mixture of Al-Cu-Fe + alloy melt

→ But the microstructure is thermally unstable

Nano composites by solid state transformation or controlled cooling for specific alloys

→ But it needs consolidation process

In-situ composites by casting

### Advanced Al alloys using quasicrystalline particles\*

High elevated temperature strength alloy : Al-Fe-Cr-Ti system.

Hot extrusion of gas atomized powder

: 400 nm sized I-phase and 500 nm sized Al grain.

$\sigma_F = 400-460$  MPa at 473 K

$\sigma_F = 350-360$  MPa at 573 K.

Excellent thermal stability : 200 h at 573 K

Ductile Al alloys : Al-Cr-Ce-Co alloys

Hot extrusion of gas atomized powder

: I-phase + Al

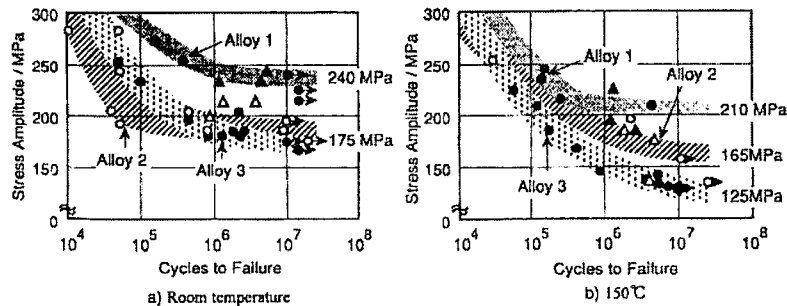
$\sigma_f = 500-600$  MPa with 12-30 % of plastic elongation

➔ Composites is a route to solve brittleness problem of I-phase

\* A. Inoue, Progress in Materials Science, 43(1998), 365



### Nanoquasicrystalline particles in Al-based system



Fatigue testing results—S-N curves (O: normal fracture; Δ: fretting fracture).

Alloy 1 : Al-4.35Cr-2.96Co-4.68Mn-3.06Zr ( $\alpha_{Al}$ +QC)

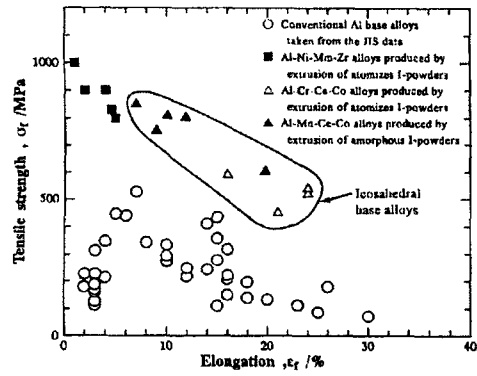
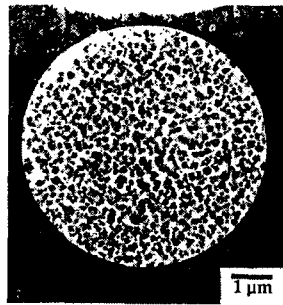
Alloy 2 : Al-4.35Cr-2.96Co-4.68Mn-3.06Zr + 5% SiC

Alloy 3 : Al-11.8Si-4.22Cu-0.63Mg

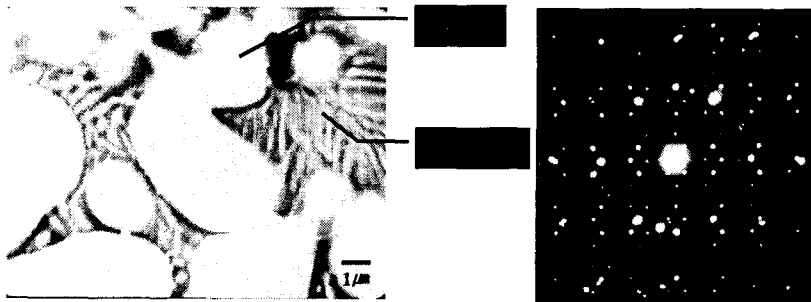


### Nanoquasicrystalline particles in Al-based system

#### ➤ Extrusion of atomized icosahedral powders

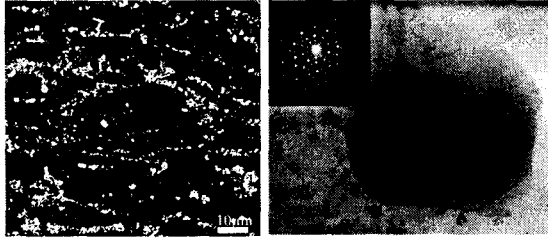


#### Typical bright field TEM image and SADP $Mg_{86}Zn_{12}Y_2$ alloy.





### Mg-Zn-Y alloys in-situ composites



Alloy	Grain size $\mu\text{m}$	Vol. fraction of 2 <sup>nd</sup> phase	Yield Stress ( $s_{0.2}$ ), MPa	UTS, MPa	Elongation %
AZ31	17.6		152	275	22.0
AZ61	9.9		175	320	19.8
AZ91	13.4		225	395	18.2
Mg <sub>96</sub> Zn <sub>3.4</sub> Y <sub>0.6</sub>	7.8	0.08	210	355	23.4
Mg <sub>95</sub> Zn <sub>4.3</sub> Y <sub>0.7</sub>	7.7	0.09	220	370	19.7
Mg <sub>94.8</sub> Zn <sub>4.3</sub> Y <sub>0.7</sub> Zr <sub>0.2</sub>	7.8	0.09	180	325	23.5

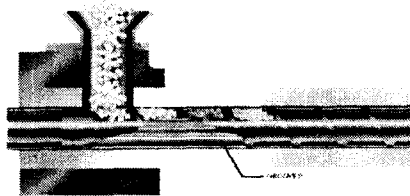


Structural	Functional
Dispersion of fine icosahedral phase in Al solid solution in Al-Li-Cu-Mg alloy (Sainfort et al., 1987)	Non-sticking quasicrystalline coatings (Dubois et al., 1991) <u>commercial cookware</u>
Precipitation of icosahedral structure in maraging steel (Nilson et al., 1998 Sandvik Steel) <u>commercial maraging steel used in razor blade and surgical tools</u>	Selective light absorber (Eisenhammer et al., 1994)
High strength Al-based alloy reinforced by nano-quasicrystalline phase (Inoue et al., 1999)	Hydrogen storage in Ti-ZrNi icosahedral quasicrystal (Kelton et al., 1997)
Polymer composite reinforced by Al-Cu-Fe quasicrystalline particles for biomedical applications (Sheares, 1999)	Thermoelectric power generation (Cyrot-Lackmann, 1997)
Quasicrystalline particles as strengthening phase in Mg-Zn-Y alloys (Kim et al., 2000)	Quasicrystals as precursor of catalyst (methanol steam reforming) (Tsal et al., 2001)



## Potential applications of QC coatings

- Plastic injection machinery : barrel and mold : low friction, no-sticking and wear properties,



- Blades in paper industry and in printer : low friction, no-sticking and wear properties,
- Metallic tubes currently used in power plant, chemical plant, petroleum plant and maritime applications to insulate and/or to protect against oxidation/corrosion.



## Powder making

- ▶ Casting and crushing
- ▶ Gas atomization
- ▶ Mechanical alloying

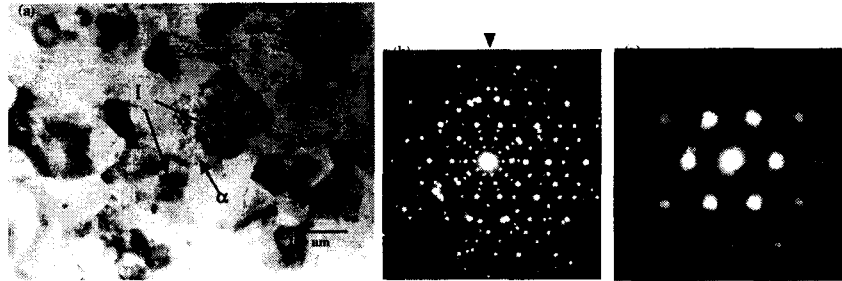
Quasicrystal formation by MA/ heat treatment

Al-Cu-Fe system : stable I phase

Ti-Zr-Ni system : stable I-phase up to around 838 K.



TEM of the bulk  $Ti_{41.5}Zr_{41.5}Ni_{17}$  sample, annealed at 807 K for 15 hrs



Formation of nanocomposites consisting of I-phase+ $\alpha$  phases.

The bulk specimen shows microhardness around 6.2 GPa and much more ductile characteristics than the single I-phase sample.

Gas atomization

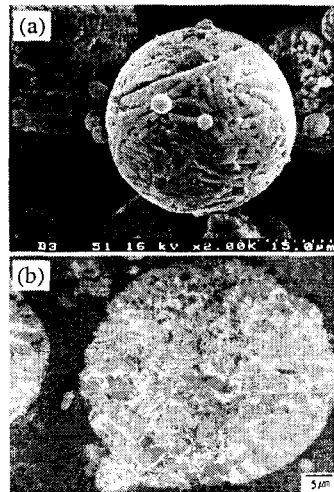
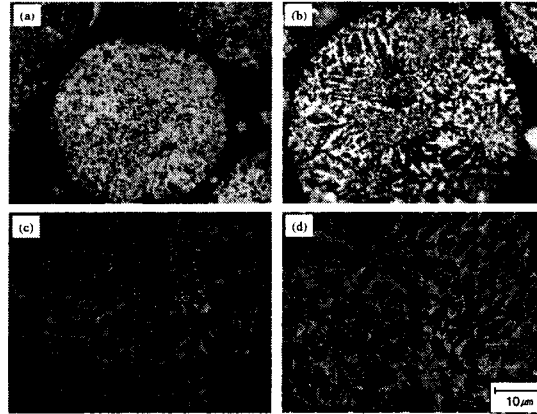
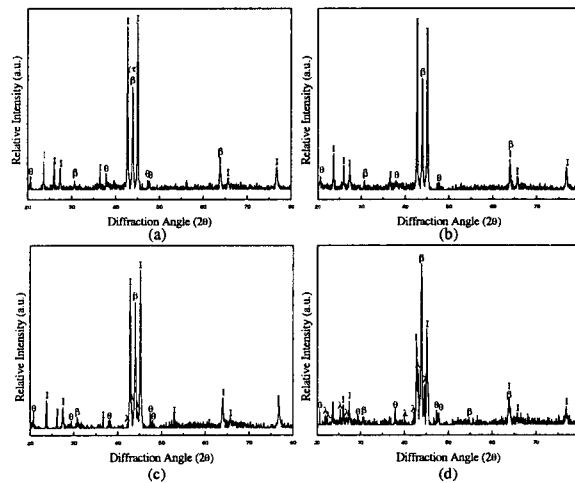


Fig. Gas atomized Al-Ni-Co-Si powder

## Microstructural change with powder size in Al-Cu-Fe powder



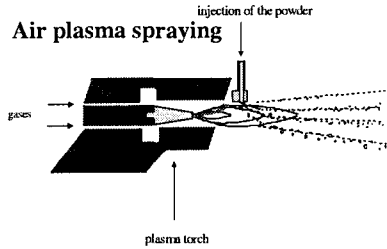
(a)+400mesh, (b)+325mesh, (c) +200mesh, and (d) +100mesh

XRD trace of  $\text{Al}_{62}\text{Cu}_{26}\text{Fe}_{12}$  gas-atomized powders

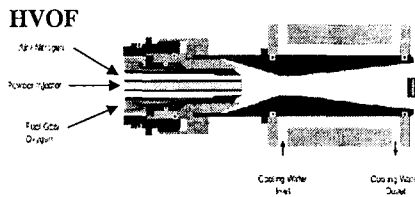
(a)+400mesh, (b)+325mesh, (c)+200mesh, and (d)+100mesh



### Comparison between APS vs. HVOF



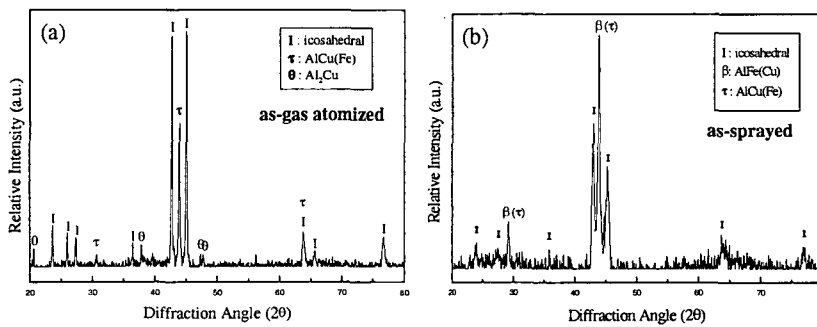
High temperature plasma ~ 15000 °C,  
 Velocity of the plasma gas ~ 650 m/s,  
 Length of plasma flame : short (~ 3 cm),  
 Large temperature gradient in particles,  
 Porosity level between 8 to 16%.



Temperature of flame zone : ~3000 °C,  
 Velocity of the gas ~2000 m/s,  
 Length of the flame : long (~20 cm),  
 Low temperature gradient in particles,  
 Porosity level less than (<5 %),  
 Wider window for process optimization.



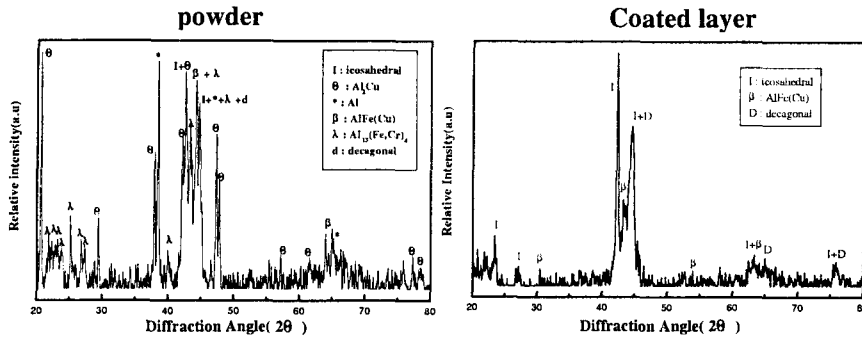
### Al loss during gas atomization and APS processes



Condition	gas-atomized powder	coating run A (300A)	standard condition (400A)	coating run B (500A)
Composition	Al <sub>62</sub> Cu <sub>26</sub> Fe <sub>12</sub>	Al <sub>59.9</sub> Cu <sub>24.5</sub> Fe <sub>15.6</sub>	Al <sub>58</sub> Cu <sub>25.7</sub> Fe <sub>15.7</sub>	Al <sub>58.5</sub> Cu <sub>25.8</sub> Fe <sub>15.7</sub>
Al recovery	99.2 %	95.8 %	93.8 %	93.6 %



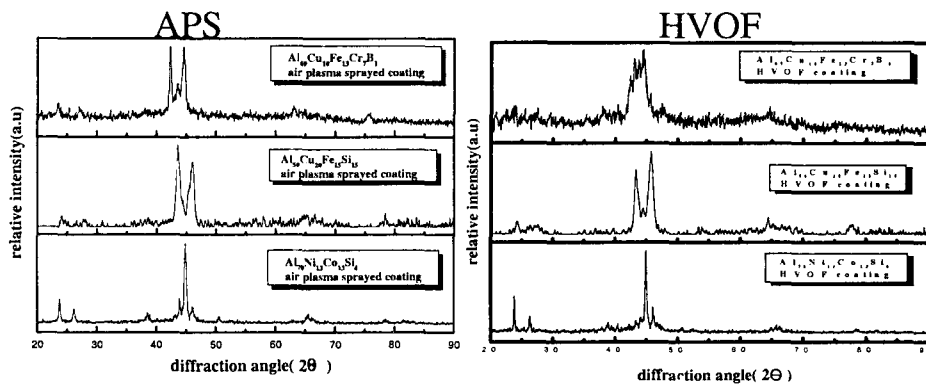
Target alloy composition :  $Al_{70}Cu_{10}Fe_{13}Cr_7$



Complex phase distribution in powders is due to excess Al content  
Coated layer consisted of expected phases



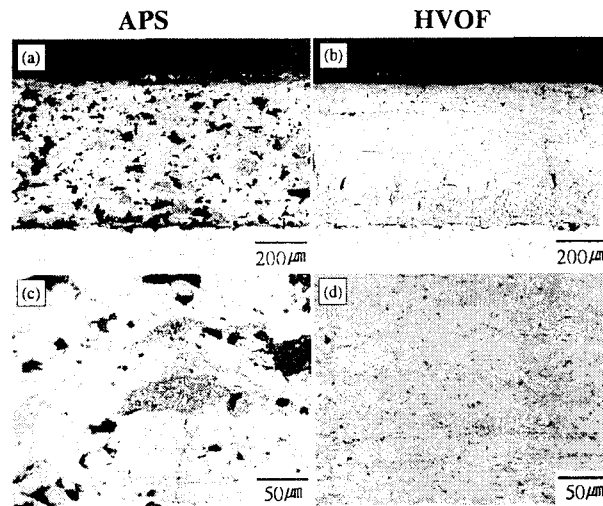
*XRD results of various specimens*



No significant difference in microstructures between APS and HVOF specimens



### Optical microstructure of Al-Cu-Fe-Si dposites



### Comparison of microstructure in APS and HVOF coatings

#### APS

Partially melted particles :  
 - large temperature gradient in powder  
 - different particle trajectories owing to the particle injection perpendicular to the plasma flame.

Porosity level : between 10 to 15 %.

Suitable for thermal barrier coating

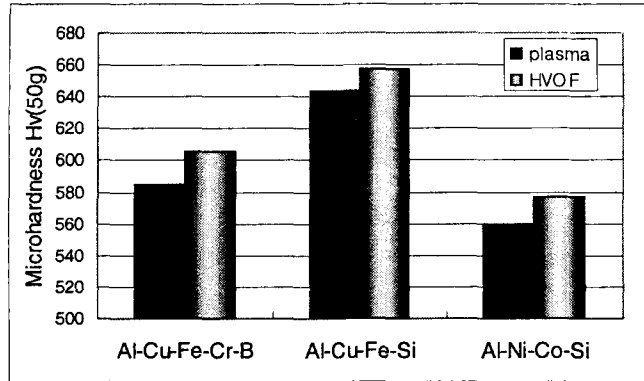
#### HVOF

- Low porosity level in coatings due to high particle velocity,  
 -small temperature gradient in particle due to long flame zone.

Porosity level : between 2 to 4 %

Suitable for wear resistance application

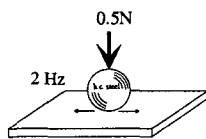
*Plasma and HVOF coatings: microhardness*



**Tribological tests**

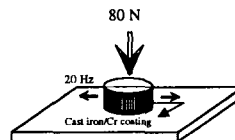
- Polishing : Ra < 0.2µm.
- ultrasonic cleaning in ethyl alcohol for 10 min.

pin-on-plate experimental device



- Load = 0.5 N, pressure = 160 MPa
  - Sliding velocity = 0.08 m/sec,
  - Sliding distance = 80 m
  - Counterpart material = high carbon steel, WC
- Small contact area

flat-on-plate experimental device



- Load = 80N, pressure = 0.7 MPa
  - Sliding velocity = 0.56 m/s,
  - Sliding distance = 560 m.
  - Counterpart material = cast iron/Cr coating
- Large contact area
- Similar contact pressure and sliding velocity to those of piston motion in auto engine.





### Why friction coefficient is so different ?

**Scratch test :**

- . ~ 0.22 (Al-Cu-Fe deposit)
- . ~ 0.19 (Al-Cu-Fe-Cr-Si deposit)
- . ~ 0.05 (Al-Cu-Fe against diamond)
- . ~ 0.15 (Al-Cu-Fe against WC)

**Pin on disk : steel ball Ø 6.3 mm**

- . ~ 0.15 (Al-Cu-Fe ingot)
- . 0.1-0.15 (Al-Cu-Fe-X deposit)

**Pin on disk : flattened ball**

- . 0.2-0.35 (Al-Cu-Fe-X deposit)

**Flat on disk : flat Ø 8 mm**

- . 0.35-0.45 (Al-Cu-Fe-X deposit)

The variation of friction coefficient is sensitive to contact area :

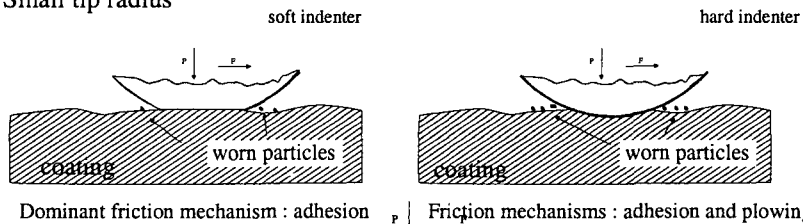
Large contact area is favorable for formation of stable intermediate layer,

Friction coefficient between two intermediate layers are measured

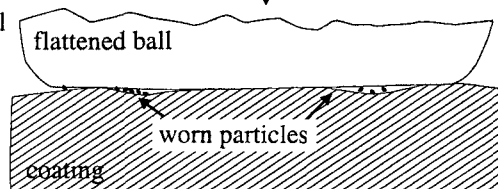


### Influence of indenter geometry and contact area on friction

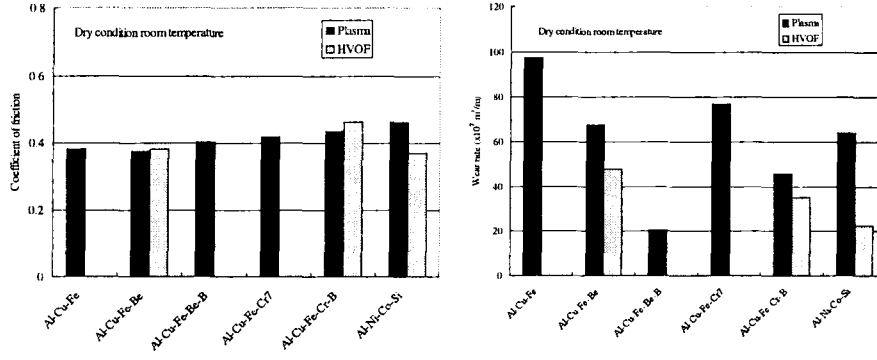
**Small tip radius**



**Flattened ball**



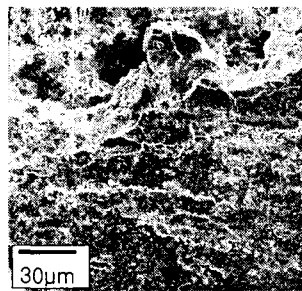
### Friction coefficients and wear rates of coatings



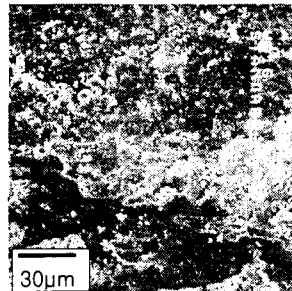
Dry condition, RT, Flat on plate

### SEM image of worn surface

Sliding direction



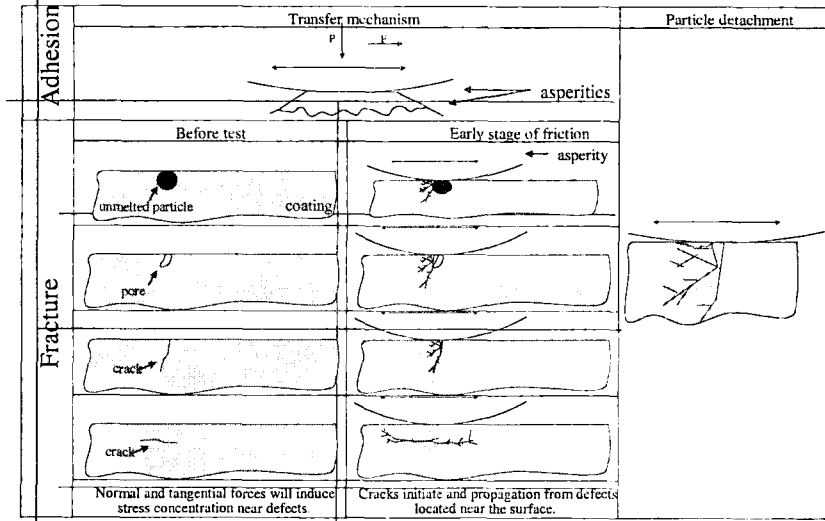
Al-Ni-Co-Si APS



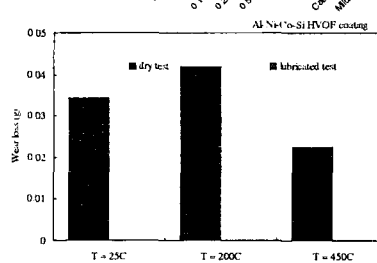
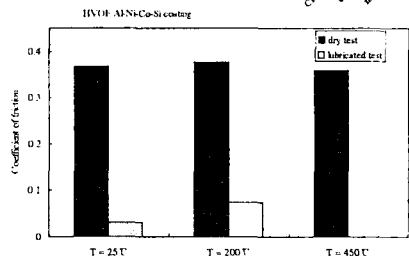
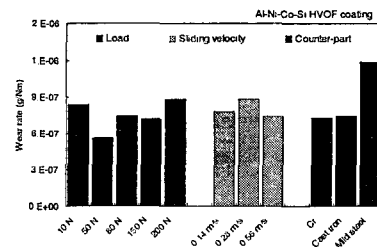
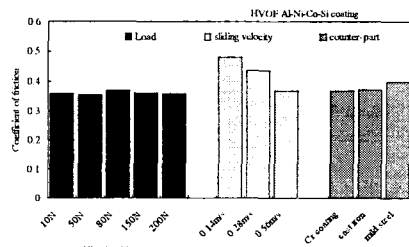
Al-Ni-Co-Si HVOF

Higher wear loss in APS coating due to high porosity and inhomogeneous microstructure

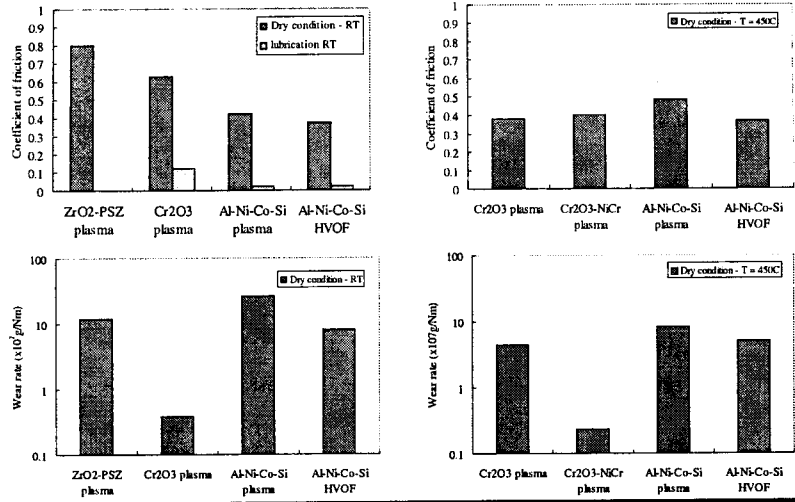
### Wear mechanisms



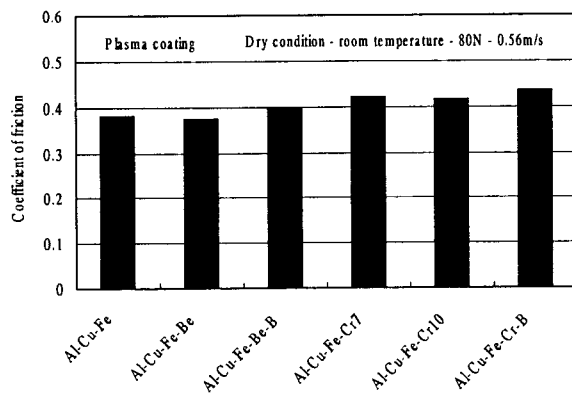
### Influence of test conditions on friction coefficients



### Comparison with ceramic coatings



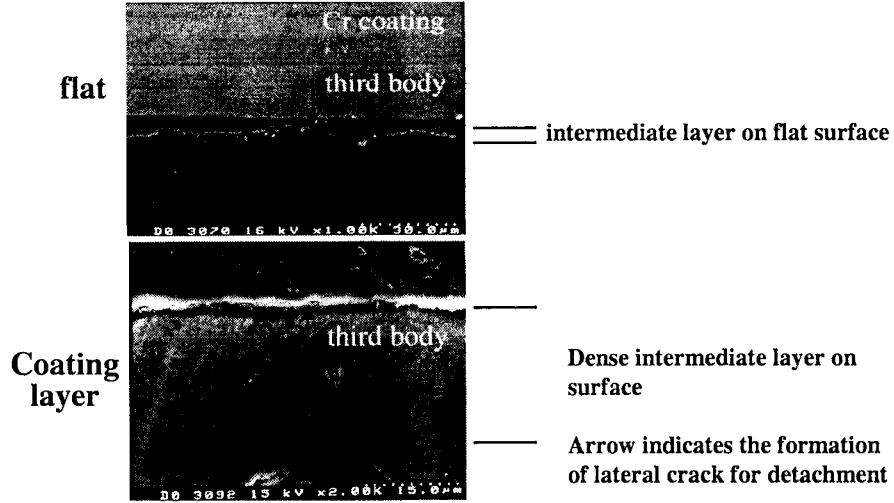
### Coefficient of friction (dry condition at RT)



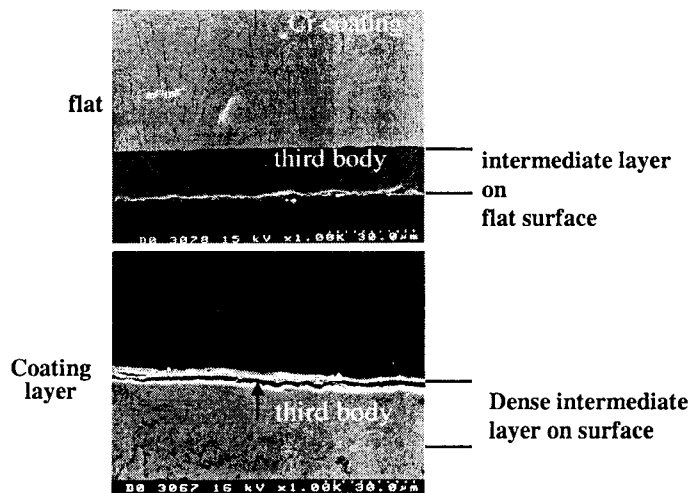
Brass	0.56
Mild Steel	0.67
SUS	0.52
Plasma PSZ	0.78
Plasma Cr <sub>2</sub> O <sub>3</sub>	0.61



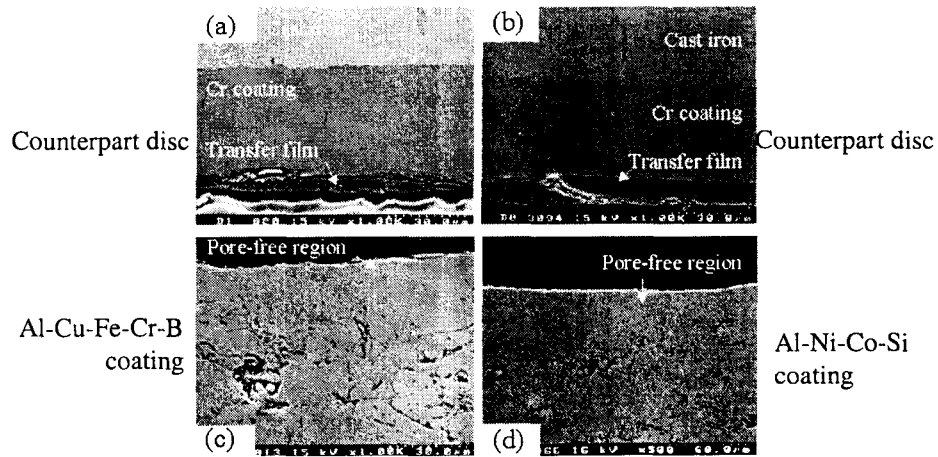
### Intermediate layer formation on flat and coating surfaces Al-Ni-Co-Si HVOF coating (at room temperature)



### Intermediate layer formation on flat and coating surfaces Al-Ni-Co-Si HVOF coating (at 450 K)



## Evolution of the contact surface after friction tests APS coatings of Al-Cu-Fe-Cr-B and Al-Ni-Co-Si alloys



## Amorphous powder coating

Amorphous structure : homogeneous, wear and corrosion resistance

Precursor to nanostructure : suitable heat treatment

Armacor powder (LMT)

Fe-Cr-B-Ni-Mo powder coating

Glass coating by twin wire arc spraying

HVOF spraying : glass fraction is very low

Super-hard steel coating (DOE's INEEL)

Fe based amorphous coating

A tough, low cost, wear and corrosion resistant coating

Hardness : up to 16 GPa

one of top 100 technologies (2001)

## Summary

1. Quasicrystalline powders shows exotic physical and mechanical properties
2. Applications :  
structural application : strengthening particles for composites  
Coating application : wear resistance, low friction coefficient
3. For thermal spaying : material loss during process should be considered to control chemical composition of deposit
4. Friction coefficient is strongly dependent on contact geometry  
Friction coefficient from pin on plate : 0.1-0.2  
Friction coefficient from flat on plate : about 0.46.
5. Quasicrystalline materials show lower friction coefficient but higher wear rate than corresponding values of  $\text{Cr}_2\text{O}_3$  coated layer.
6. Amorphous coating seems to be promising